Indian Journal of Experimental Biology
Vol. 61, March 2023, pp. 185-195
DOI: 10.56042/ijeb.v61i03.71568

Pharmacological evaluation and kinetics of *in vitro* drug release efficacy of biofabricated silver nanoparticles using medicinally important *Justicia neesii* Ramamoorthy

Yasmin Khambhaty* & Suryakiran Bondada

Microbiology Division, CSIR-Central Leather Research Institute, Adyar, Chennai – 600 020, Tamil Nadu, India

Received 12 November 2022; *revised 10 February 2023*

Green nanotechnology, the science that utilizes various plant resources for the synthesis of nanoparticles without posing any chemical hazard has proved to be highly efficient and environment friendly technique. This opens up options for the synthesis of novel nanoparticles with desirable characteristics required for various application viz., biosensors, biomedicine, cosmetics, nanobiotechnology, as antimicrobials, electronics, sensing etc. In this context, here, we have made an attempt for cost effective and eco-friendly synthesis of silver nanoparticles (AgNPs) using the extract of medicinally important plant *Justicia neesii* Ramamoorthy. The phytochemical analysis of the extract exhibited the presence of glycosides, flavonoids, lignins, phenols, phytosterols, reducing sugars, saponins, etc. The absorbance peak of the biofabricated nanoparticles at 425 nm as indicated by UV-Vis spectrophotometer broadens with increase in time indicating their poly dispersity nature and particle size analyzer revealed the average size to be in the range of 20-45 nm. The antioxidant and antimicrobial activity of the synthesized AgNPs demonstrated promising results. The kinetics of *in vitro* drug release profile of the drug loaded AgNPs was carried out and the data obtained was correlated with various mathematical models. The drug release from AgNPs at both the pH's shows good fit to the First order model which is obvious from the high values of coefficient of correlation which logically means that the release of drug from AgNPs is dependent on the concentration present within the nanoparticles.

Keywords: Antimicrobial activity, Antioxidant activity

Nanotechnology is employed as a tool to explore various avenues of medical science like imaging, sensing, targeted drug delivery, gene delivery systems and artificial implants[1]. Nanoparticles have been synthesized by several ways using chemicals as precursors and surfactants as stabilizing agents which are very expensive and cause hazard to the environment, human and biological systems[2]. Nevertheless, the engagement of biological entities for their synthesis has been reported to have tremendous advantages[3]. Among the metal nanoparticles, silver has gained much attention mainly due to its antimicrobial and pharmaceutical applications[4]. Investigations support that silver ions, metallic silver or AgNPs can be used for various applications since they pose low toxicity to human cells, high thermal stability and low volatility[5]. The antimicrobial activity of the AgNPs mainly depends on the size property. The small sized nanoparticles have large surface area to improve the antimicrobial activity in addition to improving chemical stability[6]. Plants and their parts possess carbohydrates, fats, proteins, nucleic acids, pigments and several types of secondary metabolites which act as reducing agents to fabricate nanoparticles from metal salts without producing any toxic byproducts. Siddiqi *et al.*[7] have reported green synthesis of silver nanoparticles using various plants.

In the present study, we report a facile, economical and greener route for synthesizing stable AgNPs with the bioreduction of *J. neesii* Ramamoorthy extract. *Justicia* is a plant belonging to family Acanthaceae, growing as a perennial herb in tropical regions of India. This family of plant mainly contains alkaloids, tannins, diterpenoids, cyanogenic compounds and saponins[8]. The ethnopharmacological data suggest that *Justicia* can be used for treating variety of diseases, whereas, the pharmacological tests with different species suggest that they may possess antiviral, antibacterial, antiulcer and allelopathic properties[9]. In mid last decade, synthesis of AgNPs

*Correspondence:
Phone: +91 (44) 2443 7225
E-Mail: yasmink@clri.res.in

from different species of *Justicia* plant parts and their various effects viz., cytotoxicity[10], antioxidant[11], antibacterial[12,13], biocontrol agent[14], etc., gained significance[15]. Nevertheless, the review of literature did not reveal any significant information on the said aspect particularly from *J. neesii* with an exception where the antimicrobial[16] properties of the plant extract are reported.

In the current study, we explored the use of *J. neesii* plant extract in synthesizing AgNPs and characterize them and also investigated their antimicrobial as well as antioxidant properties. Furthermore, we also studied the kinetics of *in vitro* release of doxorubicin (DOX), a major chemotherapeutic drug, in order to determine the suitable model describing the dissolution profile.

Materials and Methods

Materials

Silver nitrate ($AgNO_3$), potassium bromide (KBr) and all other chemicals were purchased from Sigma Aldrich, India. All microbiological media were purchased from Hi-Media, India. Double distilled water was used throughout the reaction.

Collection of plant and preparation of its extract

The plant samples were collected from different areas of East Godavari district, Andhra Pradesh, India during the month of January-February during day time. The whole plant parts including leaves, stem, twigs, flowers, seeds, roots were separated, made free from soil, washed thoroughly with distilled water; shade dried and coarse powdered using hand pulverizer. The powder was then extracted with ethanol by using Soxhlet apparatus at a temperature of about 50-55ºC for 8 h. The extract was concentrated using vacuum evaporator, dried in vacuum desiccator and further subjected to phytochemical analysis following standard methods[8,9].

Biofabrication of AgNP's

For the biofabrication of AgNPs, 10 g of the plant material was subjected to hot maceration method using 100 mL of double distilled water, which was then filtered through muslin cloth and eventually through Whatman No.1 filter paper; the filtrate was stored at 4ºC for future use. The synthesis of AgNPs was carried out by plant extract mediated bioreduction of $AgNO_3$ solution. Briefly, 1.0 mL of the plant extract as described above was added to 10 mL of 1 mM $AgNO_3$ solution and heated at about 60ºC with constant shaking (120 rpm) for about an hour. A change in colour from light yellow to brown was indicative of the formation of AgNPs. A negative control (only filtrate) and positive control ($AgNO_3$ solution) was also maintained with the experimental sample.

Optimization studies for the production of AgNPs

Parameters like concentration (0.5-4.0 mM) and volume (1 mM at 10 mL gradient intervals) of $AgNO_3$ solution and plant extract volume (0.25-1.5 mL) was preliminarily optimized and change in color was measured at 420 nm. Subsequently, studies on effect of other factors like pH (6.0-12.0, by adjusting with 0.1M NaOH and 0.1M HCl), temperature (40-100ºC) and time (30-180 min), on the synthesis of AgNPs was carried out. Once all the parameters were optimized, AgNPs were prepared under these conditions, centrifuged at 12,000 rpm for 30 min and thoroughly washed with de-ionized water. The obtained pellet were kept in −80ºC Ultra Refrigerator (Biocare) and further subjected to lyophilization (Penqu Classic Plus-Lyophilizer) to obtain completely dried nanoparticles for further use.

Characterization of biofabricated AgNP's

The AgNPs thus obtained were characterized using UV-Visible Spectrophotometer (JASCO V760 model) between wavelengths of 300 and 600 nm. The Fourier Transform Infra-Red (FTIR) spectra of the control and biofabricated AgNPs were recorded on Perkin Elmer C99999 Spectrometer in the range of 4000−400 cm^{-1} over 500 scan with a resolution of 2 cm^{-1}. The Scanning Electron Microscopy (SEM) and Energy Dispersive X-Ray Analysis (EDAX) were also performed to determine the size and shape of AgNPs. Thin films of the sample were prepared on carbon coated copper grid by adding a very small amount of the sample on the grid and then allowed to dry, putting it under a mercury lamp for 5 min. Thermo Gravimetric analysis (TGA) for pyrolysis was performed at 10°C min^{-1} heating rate (TGA, Q50 – TA). The isothermal behavior of AgNPs was investigated using Differential Scanning Colorimetry (DSC) over a temperature range of 50-600ºC in ambient air (DSC, Q200 – TA). Particle size distribution was studied by dynamic light scattering (DLS) measurement and zeta potential analysis on a Zetasizer (Malvern Instruments, UK). For Atomic Force Microscopy (AFM), a thin film of AgNPs was prepared on the borosilicate glass slide to analyze the surface morphology. The prepared thin film was analyzed in the tapping mode using AFM; NT-MDT Integrated Solutions for Nanotechnology.

Loading of DOX to AgNPs and studies on its *in vitro* release

For loading and release studies, the method of Madhusudhan *et al*.[17] was followed with slight modifications. Briefly, the DOX was added to AgNPs dispersion at a final concentration of 10^{-4} M and stirred at 1000 rpm for 30 min. To ensure complete loading of drug on nanoparticles, it was further incubated for 24 h at 35ºC. The mixture was eventually centrifuged at 15,000 rpm for 30 min. The pellet thus obtained was re-dispersed in de-ionized water and the DOX concentration was determined by measuring its absorbance at 480 nm. The percentage loading of DOX on AgNPs was estimated by the following formula:

$$\%\ loading = \frac{total\ amount\ of\ the\ DOX\ added - amount\ of\ DOX\ in\ solution}{total\ amount\ of the\ DOX\ added} \times 100$$

Further, the release studies were carried out at 37°C in buffer solutions maintained at pH 4.6 and pH 7.4. The drug release studies were performed in triplicate for each of the samples.

Kinetics of *in vitro* drug release

Several mathematical equations define the dissolution profile. Once an appropriate function has been selected, the evaluation of dissolution profile can be carried out and hence the drug release profile can be correlated with drug release kinetic models. In order to describe the kinetics of drug release, various models are employed using the data obtained from the *in vitro* drug release study of nanoparticles and were fitted with different kinetic equations like zero order- cumulative % release *vs*. time[18], first order- log % drug remaining *vs*. time[19], Higuchi's model- cumulative % drug release *vs*. square root of time[20] and Korsmeyer–Peppas plot- log cumulative drug released *vs*. log t[21]. The selection of best fitted kinetic model of the dissolution data was evaluated by comparing the regression coefficient (r^2) values of the models.

Pharmacological evaluation of synthesized AgNPs

2,2-diphenyl-1-picrylhydrazyl (*DPPH*) *radical scavenging activity*

The *in vitro* free radical scavenging activity was assessed using DPPH reagent[22] after slight modification. DPPH gets reduced by reaction with an antioxidant compound that can donate hydrogen and a change in color from deep violet to light yellow is observed. Briefly, a reaction mixture containing 1 mL of 0.1 mM DPPH and various concentrations of nanoparticles (20-100 µg/mL) were made up to 3 mL using deionized water and tubes were incubated for 30 min in dark. The formed yellow colour chromophore was measured at 517 nm. Butylated hydroxyl toluene (BHT) was used as a standard for comparison. The percentage of scavenging was calculated by following equation:

$$Percentage\ scavenging\ [DPPH] = \frac{Absorbance\ of\ the\ control - Absorbance\ of\ the\ sample}{Absorbance\ of\ the\ control} \times 100$$

Antimicrobial activity

The antimicrobial activity was carried out by agar well diffusion assay[23], using Gram positive, Gram negative bacteria and fungi, after slight modification. Nutrient agar and Potato Dextrose agar were prepared and sterilized by autoclaving. About 100 µL of different bacterial strains and fungi were spread on the respective media using L-rod. Subsequently, 5 mm diameter wells were bored on these plates using sterile cork borer. The respective wells were added with 20 µL of synthesized AgNPs at 50, 100 and 200 µg/ mL concentration. The content in the plates were allowed to diffuse and then incubated at 37±2°C for 24 h and fungal plates at 30±2°C for 24-48 h. Ciprofloxacin and nystatin were used as positive controls at 10 µg/well concentration to compare the antibacterial and antifungal effects, respectively. Each experiment was performed in triplicate and the zone of inhibition was noted after incubation period.

Statistical analysis

Statistical analysis of the data were carried out using Student's t-test and the results were considered significant when $P < 0.05$.

Results

Identification of plant specimen and phytochemical analysis of its extract

The plant used in the present study was taxonomically identified by the experts of Botanical Survey of India, Hyderabad (BSI/DRC/2013-14/Tech./915) as *J. neesii* Ramamoorthy (Fig. 1). The preliminary evaluation on the phytochemical characterization for occurrence of various bioactive components in the aqueous extract of *J. neesii* revealed the presence of glycosides, alkaloids, tannins, sterols, saponins and flavanoids (data not shown). Several studies justifying the occurrence of various bioactivities in the *Justicia* plant extract due

Fig. 1 — *Justicia neesii* plant used for the preparation of AgNP's

to the presence of these phytochemicals have already been detailed[9,24].

Biofabrication of AgNPs

The biofabrication of nanoparticles mainly involves oxidation/reduction reactions catalysed by microbial enzymes or plants phytochemicals and are classified under 'bottom up approach'[25]. Among all the biological sources, plant extracts are easily available, safe and usually nontoxic. They possess a variety of phytochemicals that mediate the reduction of silver ions. Water soluble components like flavones, organic acids and quinones cause immediate reduction of the ions[26]. In the present study, the biofabrication of AgNPs was carried out by reduction of silver ions with *J. neesii* extract without the aid of any chemical reducing agent. This was well visualized by change in the colour from pale yellow to dark brown within few minutes of the addition of plant extract to $AgNO_3$ solution. Metal nanoparticles exhibit different colour in solution due to their optical properties, where AgNPs exhibit brown colour attributed to the excitation of the Surface Plasmon Resonance (SPR), which play an important role in the conformation of the AgNPs formation. The wavelength at maximum peak absorbance (λ_{max}) corresponds to the SPR band and for AgNPs is normally in the range of 400-450 nm. In the current study, a steady increase in the intensity of SPR, which peaked at about 420-425 nm suggested a gradual increase in the yield of AgNPs. The control experiment without the extract remained colourless [Suppl. Fig S1. All supplementary data are available only online along with the respective paper at NOPR repository (http://nopr.res.in) as well as journal website].

Optimization of different parameters for synthesis of AgNPs

The formation of nanoparticles depends on various factors, such as concentration and volume of $AgNO_3$ solution, volume of plant extract solution, incubation

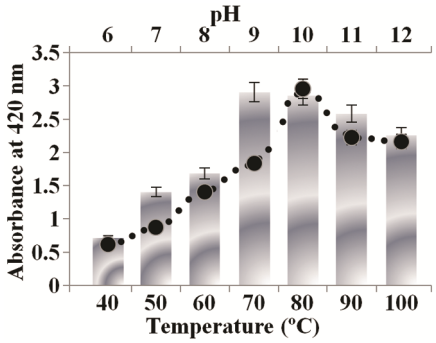

Fig. 2 — Effect of different pH and temperature on the formation of AgNP's from *J. neesii* Ramam extract

time, pH and temperature. While experimenting with different concentrations of $AgNO_3$ it was observed that the absorbance increased with the increase in concentration from 0.5 to 4.0 mM due to higher availability of silver ions for the plant extract. An increase in absorbance by almost double was observed from 0.5 and 1.0 mM concentrations for the extract, however, the increase was not very substantial in subsequent concentrations. Hence, 1.0 mM concentration of $AgNO_3$ was used for all further experiments (Suppl. Fig. S2). As far as the ratio of plant extract to $AgNO_3$ solution was concerned, 1:20 gave the best results for *J. neesii* extract, however, there was a dramatic difference between the adjacent two ratios and hence this ratio was maintained in all following experiments (Suppl. Fig. S3). Nevertheless, even when the volume of plant extract was varied, maximum nanoparticles synthesis was observed at 1:20 ratio (Suppl. Fig. S4).

pH has an important role in the synthesis of the nanoparticles, since, the shape and the size of the nanoparticles depend on it. The results of the present study indicate that acidic pH suppressed the production of the nanoparticles, however, as the pH increases the formation of the nanoparticles also increases as viewed by an increase in absorbance and narrowing of the peak from pH 8.0 to pH 10.0 (Fig. 2). The sharp peak indicates the formation of the spherical nanoparticles[27]. However, beyond this pH, the broadening of the peak is observed (Suppl. Fig. S5). At alkaline pH range, the stability of cluster distribution and colloid formation increases with a declined tendency for aggregation of the particles due to complete charging of the clusters which maximize the repulsive electrostatic interactions. Also, at elevated pH, the reaction rate will increase subsequently involving the nucleation and growth processes of smaller particles from Ag nuclei[28].

While studying the effect of temperature on the synthesis of AgNPs, an increase in its formation was observed with the increase in temperature. The absorbance band showed the broadening of the peak at the low temperature which represents the formation of larger nanoparticles. The increase in the temperature of the reaction mixture led to the fast reduction rate of the Ag^{+} and the subsequent nucleation of the silver nuclei allowing the formation of small sized AgNPs (Fig. 2 and Suppl. Fig. S6). Contact time is also reported to play an important role in the synthesis of nanoparticles. The results of the present study show that the AgNPs prepared by green synthesis are stable without aggregation and maximum formation occurs at 120 min. Even though beyond the optimum contact time the progressive hike of absorbance spectrum with SPR at 432 nm accompanied by an increase in the colour intensity was observed, nevertheless prolonged time period resulted in aggregation and broadening of the peak occurred (Suppl. Fig. S7).

Characterization of biofabricated AgNPs

UV spectroscopy is one of the most important techniques which show that SPR exists for the metal. The UV-Vis absorbance spectra for AgNPs prepared using cell free extract were obtained at multiple time intervals from the beginning of the bioreductive reaction. UV-Vis spectral analysis indicates that the SPR for the AgNPs with dark brown color were centred approximately at 425 nm.

FTIR analysis of *J. nessii* extracts and freeze dried nanoparticles were carried out to identify the possible interactions between silver and bioactive molecules, which may be responsible for synthesis and stabilization (capping material) of AgNPs (Fig. 3). FTIR spectrum reveals bands around 1650 cm^{-1} corresponds to the bending vibrations of the amide bands of the proteins; while their corresponding stretching vibrations were observed around 2900-3000 cm^{-1}. These peaks support the presence of proteins in cell-free filtrate as observed in the spectra. It is also known that interaction of protein with nanoparticle can happen either through free amine groups or cysteine residues in proteins and via the electrostatic attraction of negatively charged carboxylate groups in enzymes[29]. The bands observed in the regions of 1000-1400 can be assigned to C-N stretching vibrations of the compounds. These observations indicate the presence and binding of proteins with AgNPs which can lead to their possible stabilization. In addition, a peak around 1380 cm^{-1} in the AgNPs formed from plant extract can be attributed to an alkyl -CH_3 group. In addition, the FTIR data revealed that secondary structure of proteins has not been affected as a consequence of reaction with silver ions or binding with AgNPs. It is important to understand though, that it is not just the size and shape of proteins, but the conformation of protein molecules that plays an important role. In both AgNP solutions, prominent bands of absorbance were observed at around 1025, 1074, 1320, 1381, 1610 and 2263 cm^{-1}. The observed peaks denote -C-O-C-, ether linkages, -C-O-, germinal methyls, -C=C- groups or from aromatic rings and alkyne bonds. These bands denote stretching vibrational bands responsible for compounds like flavonoids and terpenoids and so may be held responsible for efficient capping and stabilization of obtained AgNPs.

The morphology and size of the green synthesized AgNPs studied by SEM revealed spherical nanoparticles of ~45 nm (Fig. 4). Further, the elemental composition of the samples was also determined by EDAX, which clearly reveals the presence of Ag (represented by blue peaks/ box) indicating the green synthesis of AgNPs (Inset Fig. 4). The intense signal at 3 kV strongly suggests that

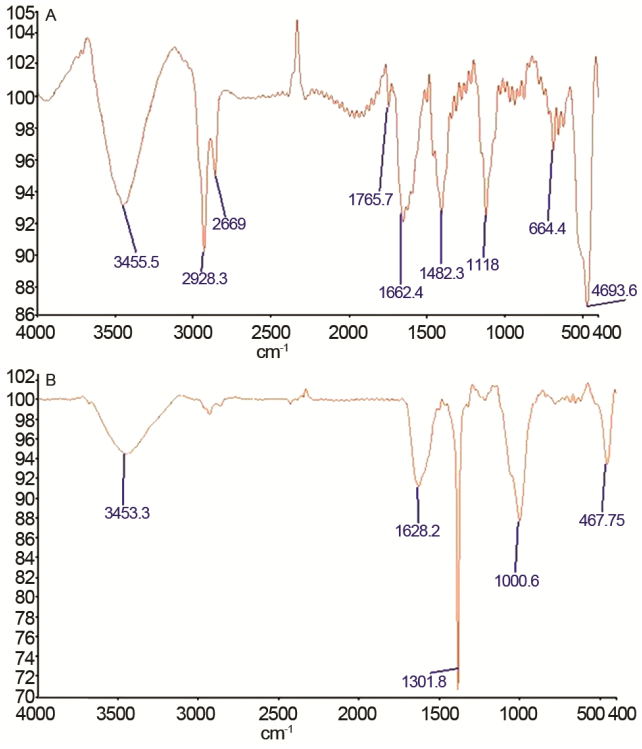

Fig. 3 — FT-IR spectra of *J. neesii* Ramam plant extract (A) and AgNP's prepared there from (B)

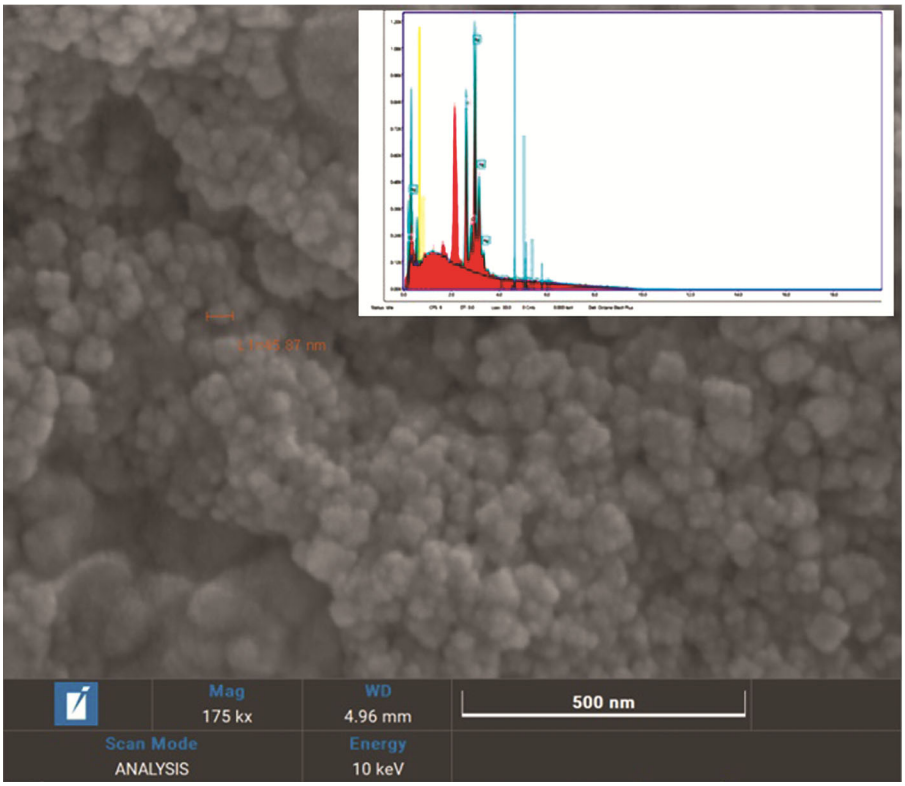

Fig. 4 — SEM and EDAX analysis of AgNP's synthesized from *J. neesii* Ramam extract

Ag was the major element, which has an optical absorption in this range due to the SPR.

The thermal stability of the nanoparticles was studied by TGA (Suppl. Fig. S8A) where the earlier weight loss could be attributed to the presence of moisture. The decomposition of the sample occurred at 272.27°C, accompanied with a weight loss of about 8% followed by a total weight loss up to 29.75% by 800°C suggesting that the organic capping compounds on the AgNPs must have decomposed. The unrecompensed residue of silver was around 70.25%. From the DSC curve (Suppl. Fig. S8B) it was observed that the AgNPs produced by *J. neesii* showed an endothermic peak at 112.75ºC. The denaturation enthalpy shows a multistage decomposition of the compound. These results showed that the compound responsible for the nanoparticles formation i.e. reduction of Ag^{+} to Ag^{0} could be thermally stable compound. The decomposition temperature by thermo gravimetric study and the denaturation temperature by the DSC curve for these nanoparticles are in good compatibility.

Surface topology of the green synthesized AgNPs were obtained with AFM in solid and in semi-contact mode. The micrographs clearly indicate that the biofabricated AgNPs possess spherical shape and

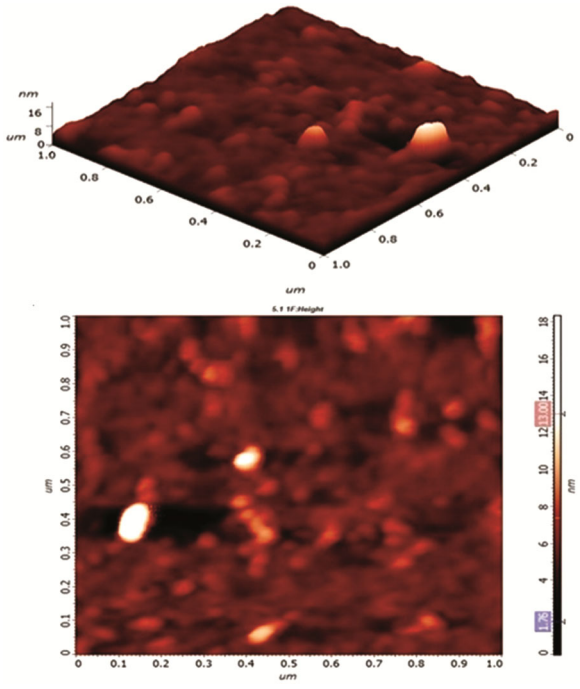

Fig. 5 — 2d and 3d AFM images showing the AgNp's synthesized from *J. neesii* Ramam extract

have the calculated sizes in the range of 16-20 nm (Fig. 5). The mean particle size diameter and polydispersity indices were all measured in solutions

directly after synthesis of the AgNPs using particle size analyzer. The size of the colloidal AgNPs and their granulometric distribution was recorded, expressed against the particle number and their occupied volume. The data illustrated that the size of the particles was between 50-70 nm for *J. neesii* AgNPs (Fig. 6). The Zeta potential values were measured and found to fall at −17.2 ± 8.28 mV for the AgNPs synthesized from *J. neesii* extract. This value shows full stabilization of the nanoparticles in addition to their narrow size distribution and provides satisfactory evidence about their little tendency towards aggregation. This behaviour clearly suggests the presence of strong electric charges on the particles' surfaces to hinder agglomeration. The value on the negative side is also indicative of the efficiency of the capping materials in stabilizing the nanoparticles by providing intensive negative charges which keep all the particles away from Reddick threshold[30]. It is unanimously accepted that charged particles can interact across long distances via electrostatic repulsive forces leading to a disruption in the surface charge as a way to induce nanoparticles assembly by modifying the condition of the reaction[31].

Loading of doxorubicin to AgNPs and study on kinetics of release data

The percentage loading efficiency of the drug to the nanoparticles synthesized from *J. neesii* extract

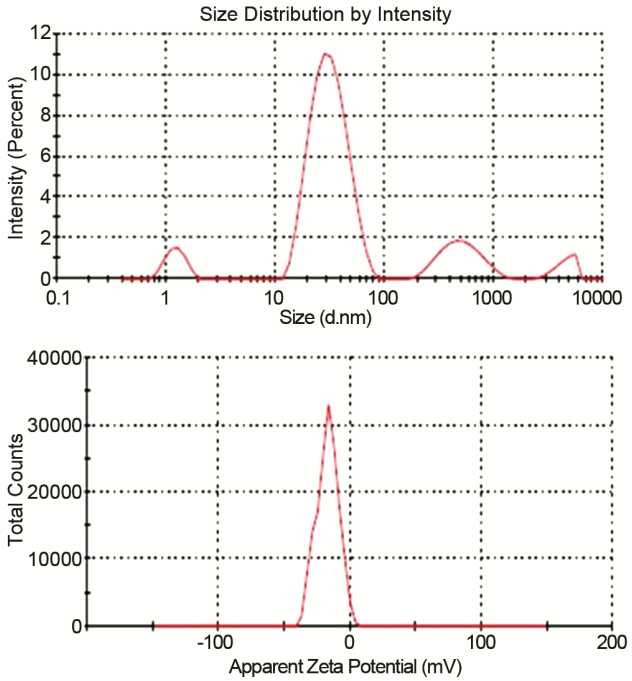

Fig. 6 — Particle size distribution and zeta potential of the AgNP's synthesized from *J. neesii* Ramam *extract*

was found to be 74.8% at acidic pH and negligibly less at alkaline pH as calculated from the above-mentioned formula. In order to measure the release of DOX loaded onto AgNPs, it was exposed to acidic (acetate buffer- pH 4.6) and physiological (phosphate buffer- pH 7.4) conditions at 37°C. As observed from Suppl. Table S1, the pH of the medium strongly influenced the rate and amount of DOX released from the DOX loaded AgNPs. Comparatively much faster DOX release at pH 4.6 was observed than at pH 7.4. At the end of 12 h, 92.27% ± 3.2%, 10.46% ± 2.2% of DOX was released in acetate and phosphate buffer, respectively for *J. neesii* – DOX@AgNPs. The efficacy of DOX loaded nanoparticles as delivery system may be improved due to its pH dependent release without disturbing the normal cells[32].

The *in vitro* drug release profile was fitted in different models and evaluated by correlation coefficient (r^2) where the highest degree of correlation coefficient determines the suitable model that follows drug release kinetics. A system is defined to be of zero order kinetics if the process is of constant drug release from the matrix and is independent of the drug concentration. This model was applied to the release profile of drug loaded AgNPs and evaluated (Suppl. Fig. S9). The obtained analysis indicates that drug release from the AgNPs does not follow the principle of zero order release kinetics due to comparatively lower values of R^2 (0.882 for pH 4.6 and 0.907 for pH 7.4). The drug release which follows first-order kinetics can be studies by plotting the log percentage of drug remaining *vs*. time where the slope of the plot gives the first-order rate constant[33]. From the data obtained, it is observed that the drug release from AgNPs at both the pH shows good fit to this model which is indicative of the high values of coefficient of correlation (0.938 for pH 4.6 and 0.981 for pH 7.4) (Fig. 7A). This logically means that the release of drug from AgNPs is dependent on the concentration present within the nanoparticles. The release experimental data obtained were also fitted into Higuchi model and is represented at Fig. 7B. The results indicated the drug release from nanoparticles matrix at both the pH's showed the best fit and followed Higuchi drug release kinetics as evident from high R^2 values (0.974 for pH 4.6 and 0.961 for pH 7.4). In the current study, the diffusion mechanism of the drug release was confirmed by Korsmeyer–Peppas plots with R^2 values 0.986 and 0.969 for pH 4.6 and pH 7.4, respectively and the gradient values (n) 0.606 and 0.568 (Suppl. Fig. S10) which falls

between 0.42 < n < 0.85. The values of the slopes indicated that the drug release followed an anomalous transport or non-Fickian diffusion transport, which means that the diffusion is time dependent and the release for drug from the AgNPs is dependent on the concentration of the drug thus supporting the first-order reaction theory[34].

Pharmacological evaluation of synthesized AgNPs

Antioxidant activity

The DPPH activity is commonly used antioxidant assay for analyzing the free radical scavenging active compounds. The antioxidant activity of AgNPs fabricated in the present study by DPPH radical scavenging method showed significant inhibition of free radicals of about 77% at 100 µg/mL concentration (Table 1). The AgNPs of *J. neesii* showed a low IC_{50} value of 51.79 µg/ mL as compared to standard BHT which showed an IC_{50} value of 60.89 µg/mL, thus exhibiting a high antioxidant activity. In another study, the ethanolic extract of whole plant of *J. neesii* was screened for elucidating its antioxidant potential and exhibited good antioxidant nature and reducing ability. The IC_{50} value against DPPH was found to be 55.72 µg/mL[16].

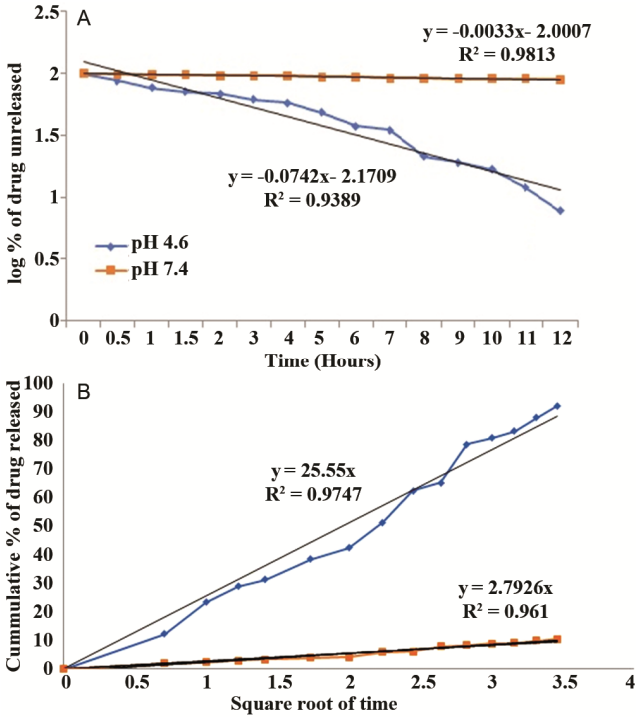

Fig. 7 — (A) First order plots; and (B) Higuchi's plots of drug release kinetics loaded onto AgNP's synthesized from *J. neesii* Ramam extract at pH 4.6 and pH 7.4

Antimicrobial activity

The antimicrobial activity of AgNPs synthesized using *J. nessii* extract was investigated against various Gram positive and negative bacteria viz., *Staphylococcus aureus*, *Bacillus subtilis*, *Micrococcus* sp., *Pseudomonas aeruginosa*, *Escherichia coli* and *Klebsiella pneumoniae* using the well diffusion method. All the tested strains exhibited significant zone of inhibition indicating the efficacy of the biofabricated AgNPs. These were also tested against three fungi viz., *Aspergillus niger*, *Aspergillus flavus* and *Penicillium chrysogenum* (Table 2). Earlier studies on the antimicrobial nature of ethanolic extract of *J. neesii* showed significant antibacterial activity compared to ciprofloxacin. The maximum Activity Index (AI) was observed against *K. pneumonia* (1.208) and low AI value for *S. faecalis* (0.963) compared to other bacterial species. However, Gram positive bacteria exhibited an overall maximum zone of inhibition as compared to Gram negative bacteria[23].

Table 1 — Antioxidant activity AgNP's fabricated from *Justicia neesii* extract

Concentration (µg/ mL)	% inhibition	
	BHT	*J. neesii* AgNPs
20	13.98±0.14	22.99±0.26
40	31.11±0.25	38.59±0.34
60	48.06±0.21	52.03±0.19
80	61.14±0.36	65.19±0.48
100	73.31±0.35	77.01±0.24

[Values are expressed in mean; n=3]

Table 2 — Antimicrobial activity [Zone of inhibition (mm)] of AgNP's biofabricated using *Juscticia neesii* extract

Treatment	Test organism								
	Staphylococcus aureus	*Bacillus subtilis*	*Micro-coccus*	*Pseudomonas aeruginosa*	*Klebsiella pneumoniae*	*E. coli*	*Aspergillus niger*	*A. flavus*	*Penicillium chrysogenum*
Ciprofloxacin/Nystatin (10 µg/well)	22.0±0.3	20.0±0.4	19.0±0.6	18.0±0.4	17.0±0.3	18.0±0.2	23.0±0.1	22.0±0.2	20.0±0.1
J. neesii Ramam. AgNPs (50 µg/well)	8.1±0.2	12.6±0.1	9.2±0.3	8.6±0.3	6.5±0.2	7.5±0.4	7.0±0.4	9.0±0.2	7.1±0.4
J. neesii Ramam. AgNPs (100 µg/well)	10.2±0.5	14.6±0.3	10.5±0.4	10.4±0.2	7.9±0.3	9.1±0.4	9.0±0.2	10.0±0.3	8.5±0.2
J. neesii Ramam. AgNPs (200 µg/well)	11.1±0.3	15.2±0.2	10.9±0.2	11.6±0.3	8.1±0.2	10.5±0.4	11.8±0.1	12.2±0.1	10.3±0.1

[Values are expressed in mean; n=3]

The results of the present study were also in line with those of antibacterial activity of AgNPs from Vasaka (*J. adhatoda* L.) leaf extract[15]. The results of this study indicate that the green synthesized AgNPs were able to control the multidrug resistant pathogenic bacteria and hence could be used in the medical field[35].

Discussion

The facile synthesis of AgNPs from *J. neesii* plant extract has been reported. The phytochemicals/ secondary metabolites in plants are regarded as reducing agents in the green synthesis. Additionally, these are also linked to be responsible for imparting biological activities such as antioxidant, antibacterial, anticancer and antidiabetic[36]. The parameters optimized for maximum synthesis were much in line with the earlier studies. The pH and temperature were observed to have a profound effect on the formation of AgNPs. The capacity of the phytochemicals to reduce Ag^{+} to Ag^{0} increases upon addition of the hydroxide ions to the solution. Nevertheless, at high alkaline pH, the absorbance peak shifted towards longer wavelengths. As for temperature, higher temperatures resulted in peak broadening due to an increase in the concentration of nanoparticles which led to aggregation being more favorable than dispersion hence peak broadening with a shift towards longer wavelength was observed[37]. As for the release studies, much faster release of drug was observed in the present study at acidic pH. Hyperactive and fast spreading tumors exhibit amazingly increased metabolic rate, thereby causing a dearth of oxygen and nutrients, leading to attain extra energy from glycolysis, causing an acidic environment[38]. The acidic environment in the endosome possibly prompts rapid release of DOX and thereby enhancing the cell cytotoxicity[39]. Negligible amount of DOX release at physiological pH, will lead to reduce toxicity of DOX to the normal tissue, since the pH of body fluids is maintained around pH 7.4[40,41]. The DOX-loaded AgNPs are anticipated to accumulate in the tumor tissue favorably through the EPR (Enhanced Permeability and Retention) effect. Once in the tissue, the DOX@ AgNPs are believed to be internalized via tumor cells and placed in the acidic endosomal compartments, which can help to provide sufficient level of DOX, that could be separated from the AgNPs and eventually diffuse into the cytosol and then to the nucleus[42].

The free radical scavenging activities of biosynthesized AgNPs against DPPH, could be attributed to the bioactive constituents of plant extract that adhered to the spherical shaped nanoparticles and simultaneously may serve as antioxidants via transferring of a single electron and hydrogen atom[43]. The higher scavenging activities of biosynthesized AgNPs could be due to the simultaneous action of phenolic compounds as antioxidant agents and silver ions as a catalyst[44].

Earlier studies mention that the bactericidal effect could be the result of an electric charge on the surface of AgNPs, oxidative stress induction, metal ion release, or non-oxidative mechanisms that can occur simultaneously[15,45]. Additionally, certain studies have proposed that AgNPs prompt neutralization of the surface electric charge of the bacterial membrane and change its penetrability, ultimately leading to bacterial death[46].

Conclusion

Keeping the bio-mimicing process in mind, we made an attempt to fabricate AgNPs using a medicinally important *Justicia neesii* plant extract as capping and reducing agent. The concentration and physical conditions were found to affect the maximum yield, rate of the synthesis and size of the nanoparticles produced. The detailed characterization of the biofabricated AgNPs revealed the average particle size to be in the range of 20-40 nm. From the studies on kinetics of drug release data, it was inferred to follow First order plot. Further, the data also indicated that the drug release followed Non-Fickian Anomalous Diffusion (Mixed order) mechanism as revealed from Higuchi's plot and Peppa's plot. The synthesized AgNPs exhibited high antioxidant and antimicrobial potential thus giving them an edge over other materials for their potential application in medical field. This size controlled, ecofriendly and inexpensive method for the synthesis of AgNPs could be a viable alternative over other traditional methods. Moreover, the dual advantage exhibited i.e., the effective uptake of DOX loaded AgNPs at physiological pH and response at intracellular acidic pH gives them a benefit of doubt as an ideal drug delivery system to target cancer cells.

Conflict of interest

Authors declare no competing interests.

References

1 Sim S & Wong NK, Nanotechnology and its use in imaging and drug delivery. *Biomed Rep*, 14 (2021) 1.

2 Xu L, Wang YY, Huang J, Chen CY, Wang ZX & Xie H. Silver nanoparticles: Synthesis, medical applications and biosafety. *Theranostics*, 10(20) (2020) 8996.

3 Zhang D, Ma XL, Gu Y, Huang H & Zhang GW. Green synthesis of metallic nanoparticles and their potential applications to treat cancer. *Front Chem*, 8 (2020) 799.

4 Zhang XF, Li ZG, Shen W & Gurunathan S, Silver nanoparticles: Synthesis, characterization, properties, applications, and therapeutic approaches. *Int J Mol Sci*, 17 (2016) 1534.

5 Rai M, Yadav A & Gade A, Silver nanoparticles as a new generation of antimicrobials. *Biotech Adv*, 27 (2009) 76.

6 Anees Ahmad S, Das SS, Khatoon A, Tahir Ansari M, Afzal M, Saquib Hasnain M & Nayak AK, Bactericidal activity of silver nanoparticles: A mechanistic review, *Mater Sci Energy Technol*, 3 (2020) 756.

7 Siddiqi KS, Husen A & Rao RAK, A review on biosynthesis of silver nanoparticles and their biocidal properties. *J Nanobiotechnol*, 16 (2018) 14.

8 Evans WC & Saunders WB,*Trease and Evans Pharmacognosy*. 15th ed.(Cambridge University Press, London), 2002,35.

9 Geone M, Correa Antonio F & Alcantara C, Chemical constituents and biological activities of species of *Justicia* - A review. *Rev Bras Farmacogn*, 22 (2012) 220.

10 Kudle KR, Donda MR, Kudle MR, Merugu R, Prashanthi Y & Rudra MPP, Investigation on the cytotoxicity of green synthesis and characterization of silver nanoparticles using *Justicia adhatoda* leaves on human epitheloid carcinoma cells and evaluation of their antibacterial activity. *Int J Drug Dev Res*, 6 (2014) 975.

11 Ponvel K, Narayanaraja T & Prabakaran J, Biosynthesis of silver nanoparticles using root extract of the medicinal plant *Justicia adhatoda*: Characterization, electrochemical behavior and applications. *Int J Nano Dimens*, 6 (2015) 339.

12 Bose D & Chatterjee S, Antibacterial activity of green synthesized silver nanoparticles using. Vasaka (*Justicia adhatoda* L.) leaf extract. *Indian J Microbiol*, 55 (2015) 163.

13 Bharathi D, Ramalakshmi S, Kalaichelven PT & Akilakalaichelvan, Biological synthesis of silver nanoparticles by using leaf extract of *Justicia adhatoda*. *Der Pharmacia Lett*, 7 (2015) 391.

14 Bernardo-Mazariegosa, E, Valdez-Salas B, González-Mendozaa D, Abdelmoteleb A, Camachoa OT, Duran CC & Gutiérrez-Micelic F, Silver nanoparticles from *Justicia spicigera* and their antimicrobial potentialities in the bio-control of food borne bacteria and phytopathogenic fungi. *Rev Argent Microbiol*, 51 (2019) 103.

15 Thirumagai N & Pricilla Jeyakumari A, Structural, optical and antibacterial properties of green synthesized silver nanoparticles (AgNP's) using *Justicia adhatoda* L. leaf extract. *J Clust Sci*, 31 (2020) 487.

16 Sridhar N, Duggirala SL & Puchchakayala G, Antimicrobial activity of ethanolic extracts of *Justicia neesii. Bangladesh J Pharmacol*, 9 (2014a) 624.

17 Madhusudhan A, Reddy GB, Venkatesham M, Veerabhadram G, Kumar DA, Natarajan S, Yang MY, Hu A, & Singh SS. Efficient pH dependent drug delivery to target cancer cells by gold nanoparticles capped with carboxymethyl chitosan. *Int J Mol Sci*, 15 (2014) 8216.

18 Hadjiioannou TP, Christian GD, Koupparis MA & Macheras PE, *Quantitative calculations in pharmaceutical practice and research*. (VCH publishers Inc., New York), 1993, 345.

19 Bourne DWA, Pharmacokinetics. In: *Modern Pharmaceutics*, 4th edn. (Eds. Banker GS & Rhodes CT; Marcel Dekker Inc, New York), 2002, 67.

20 Higuchi T, Mechanism of sustained action medication. Theoretical analysis of rate of release of solid drugs dispersed in solid matrices. *J Pharm Sci*, 52 (1963) 1145.

21 Korsmeyer RW, Gurny P, Delker EM, Buri P & Peppas NA, Mechanism of solute release from porous hydrophilic polymers. *Int J Pharm*, 15 (1993) 25.

22 Olugbami JO, Gbadegesin MA & Odunola OA. *In vitro* free radical scavenging and antioxidant properties of ethanol extract of *Terminalia glaucescens*. *Pharmacogn Res*, 7 (2015) 49.

23 Bonev B, Hooper J & Parisot J, Principles of assessing bacterial susceptibility to antibiotics using the agar diffusion method. *J Antimicrob Chemother*, 61 (2008) 1295.

24 Prabhu S & Poulose EK, Silver nanoparticles: Mechanism of antimicrobial action, synthesis, medical applications, and toxicity effects. *Int Nano Lett*, 2 (2012) 32.

25 Kota S, Dumpala P, Anantha R, Verma MK & Kandepu S, Evaluation of therapeutic potential of the silver/silver chloride nanoparticles synthesized with the aqueous leaf extract of *Rumex acetosa*. *Sci Rep*, 7 (2017) 11566.

26 Lee SH & Jun BH, Silver nanoparticles: Synthesis and application for nano medicine. *Int J Mol Sci*, 20 (2019) 865.

27 Meva FE, Segnou ML, Ebongue CO, Ntoumba AA, Kedi PBE, Deli V, Etoh M & Mpondo EM, Spectroscopic synthetic optimizations monitoring of silver nanoparticles formation from *Megaphrynium macrostachyum* leaf extract, *Rev Bras Farmacogn*, 26 (2016) 640.

28 International Standard Methods for Determination of Particle Size Distribution Part 8: Photon Correlation Spectroscopy. (International Organization for Standardization ISO), 13321 (1996) 19.

29 Elamawi RM, Al-Harbi RE & Hendi AA, Biosynthesis and characterization of silver nanoparticles using *Trichoderma longibrachiatum* and their effect on phytopathogenic fungi. *Egypt J Biol Pest Control*, 28 (2018) 28.

30 Riddick TM, Control of colloid stability through zeta potential: With a closing chapter on its relationship to cardiovascular disease. (Zeta-Meter Inc., VA, USA.,), 1968.

31 Salem HF, Eid KAM & Sharaf MA, Formulation and evaluation of silver nanoparticles as antibacterial and antifungal agents with a minimal cytotoxic effect. *Int J Drug Dev*, 203 (2011) 293.

32 Navya PN, Kaphle A, Srinivas SP, Bhargava Sk, Rotello VM & Daima HK, Current trends and challenges in cancer management and therapy using designer nanomaterials. *Nano Converg*, 6 (2019) 23.

33 Dash S, Murthy PN, Nath L & Chowdhury P, Kinetic modeling on drug release from controlled drug delivery systems. *Acta Pol Pharm*, 67 (2010) 217.

34 Unagolla JM & Jayasuriya AC, Drug transport mechanisms and *in vitro* release kinetics of vancomycin encapsulated chitosan-alginate polyelectrolyte microparticles as a controlled drug delivery system. *Eur J Pharm Sci*, 114 (2018) 199.

35 Sangu V, Yamuna T, Anu Preethi G & Sineha A, Green synthesis and characterization of silver nanoparticles using ethanolic extract of *Mimosa pudica* linn leaves. *Indian J Chem Technol*, 28 (2021) 479.
36 Shalaby EA, Shanab SMM, El-Raheem WMA & Hanafy EA, Biological activities and antioxidant potential of different biosynthesized nanoparticles of Moringa oleifera. *Sci Rep*, 12 (2022) 18400.
37 Netai MM, Cecilia G, Munyaradzi M, Upenyu G & Stephen N, Synthesis of silver nanoparticles using plant extracts from *Erythrina abyssinica* aerial parts and assessment of their anti-bacterial and anti-oxidant activities. *Results Chem*, 4 (2022) 100402
38 Pelicano H, Martin D, Xu R, & Huang P. Glycolysis inhibition for anticancer treatment. *Oncogene*, 25 (2006) 4633.
39 Varukattu N B, Vivek R, Rejeeth C, Thangam R, Ponraj T, Sharma A, & Soundarapandian K. Nanostructured pH-responsive biocompatible chitosan coated copper oxide nanoparticles: A polymeric smart intracellular delivery system for doxorubicin in breast cancer cells. *Arab J Chem*, 13 (2020) 2276.
40 Zhao N, Woodle MC & Mixson AJ. Advances in delivery systems for doxorubicin. *J Nanomed Nanotechnol*, 9 (2018) 519.
41 Sunil P, Goldie O, Ashmi M, Ritu S, Mukesh T & Madhuri S, Folic acid mediated synaphic delivery of doxorubicin using biogenic gold nanoparticles anchored to biological linkers. *J Mater Chem B*, 11 (2013) 361.
42 Prabaharan M, Grailer JJ, Pilla S, Steeber DA & Gong SQ, Gold nanoparticles with a monolayer of doxorubicin-conjugated amphiphilic block copolymer for tumour-targeted drug delivery. *Biomaterials*, 30 (2009) 5757.
43 Demirbas A, Bafail A, Ahmad W & Sheikh M, Biodiesel production from non-edible plant oils. *Energy Explor Exploit*, 34 (2016) 290.
44 Mohanta YK, Panda SK, Jayabalan R, Sharma N, Bastia AK & Mohanta TK, Antimicrobial, antioxidant and cytotoxic activity of silver nanoparticles synthesized by leaf extract of *Erythrina suberosa* (Roxb.). *Front Mol Biosci*, 4 (2017) 14.
45 Abbas A, Ghahramani Y, Gholami A, Hemmateenejad B, Dorostkar S, Nabavizadeh M & Shargui H, The effect of charge at the surface of silver nanoparticles on antimicrobial activity against Gram-positive and Gram-negative bacteria: A preliminary study. *J Nanomat*, 720654 (2015).
46 Wang L, Hu C & Shao L, The antimicrobial activity of nanoparticles: Present situation and prospects for the future. *Int J Nanomed*, 12 (2017) 1227.